Uluslararası İleri Doğa Bilimleri ve Mühendislik Araştırmaları Dergisi
Sayı 7, S. 34-41, 10, 2023

Araştırma Makalesi

IJANSER
https://alls-academy.com/index.php/ijanser
ISSN: 2980-0811

International Journal of Advanced Natural Sciences and Engineering Researches
Volume 7, pp. 34-41, 10, 2023

Research Article

3-Dimensional High Gain High Isolation Ultra-Wide Band Antenna Array with PRS Layer

Ali Ahmad[*], Rashid Saleem[2] and Muhammad Farhan Shafique[3]

[1]*Department of Telecommunication Engineering, U.E.T Taxila, Pakistan*
[2]*Department of Telecommunication Engineering, U.E.T Taxila, Pakistan*
[3]*Center for Advanced Studies in Telecommunication, COMSATS, Islamabad, Pakistan*

[*]*(ali.ahmad3@students.uettaxila.edu.pk)*

(Received: 13 October 2023, Accepted: 22 October 2023)

(2nd International Conference on Recent Academic Studies ICRAS 2023, October 19-20, 2023)

ATIF/REFERENCE: Ahmad, A., Saleem, R. & Shafique, M. F. (2023). 3-Dimensional High Gain High Isolation Ultra-Wide Band Antenna Array with PRS Layer. *International Journal of Advanced Natural Sciences and Engineering Researches*, 7(10), 34-41.

Abstract **–** This paper presents a 3-dimensional, Ultra-wide band MIMO array antenna for high gain (M2M) communication environments. This antenna supports Ultra-Wide band (3.2GHz-10.5GHz) frequencies. The radiating patch is made from 1.6mm thick FR-4 substrate. To increase the isolation between radiating elements, parasitic structures are used. The parasitic structures are placed alongside feedline as well as radiating elements. A Defective ground plane is implemented to increase bandwidth and radiation coefficient of array. A Partial Reflecting Surface (PRS) layer, also fabricated on a similar FR-4 substrate is used above the antenna layer to improve the antenna's gain and bandwidth. More crucially, the suggested PRS antenna improves gain by 3dB average over entire ultra-wide band. Based on simulation and measurement results, this configuration appears to be a viable contender for Machine-to-Machine(M2M) communication.

Keywords – PRS, Machine-to-Machine Communication, UWB, Defective Ground Plane, Fabry-Perot Cage, MIMO

I. INTRODUCTION

(IoT)Internet of things and (M2M) Machine to Machine communication has enhanced significance for high data rate transmission techniques in wireless industry. [1] These communications require a solution allowing several devices to communicate independently with each other. To achieve a reliable data link to be established, antenna systems are necessary which can easily provide multiband access. So, the leading concentration of recent research in wireless technology is to achieve the maximum data rate possible maintain minimum resource use and have minimum effect on surrounding wireless standards. [2] In this regard Multi Input Multi Output (MIMO) technology in ultra-wide band applications has received much attention over the last few years.

The Ultra-Wideband communication band spectrum of 3.5 to 10.5 GHz interferes with other wireless spectrums. which contain a variety of frequency bands such as W-L.A.N, Wi-M.A.X, and X-band. [3] As a result, the likelihood of other communication devices causing distortion in the UWB frequency is substantially higher. However, miniaturization of system is the main restraint in deployment of UWB-MIMO communication. Un desired mutual coupling produced by miniaturization of structures reduces desirability of this technique. As a result, in MIMO systems, an

effective isolating/decoupling structure is necessary to create decoupling between antenna elements. [4]

Several MIMO antennas design with decoupling structures have been documented in the literature to provide excellent isolation between radiating elements. Numerous designs with band-notch in frequency band are reported in the existing literature to achieve interference mitigation in UWB communication. [5] These proposed antennas, on the other hand, have permanent band-notching. Even if no competing narrow band system is operating in near proximity, using the entire UWB spectrum may not be practicable for the sake of interference-free communication. As a result, antennas with defected ground structure are sought for improving UWB system performance. [6]

Many approaches for reducing mutual-coupling have recently been published. The decoupling-system between the radiating structures, which can be made up of physical elements [4] , transmission feed lines [7], and inter-coupled resonators [8] can efficiently decrease mutual coupling. To modify the transmission characteristics between radiating elements, several reported approaches use a modified ground structure [9]. In [10]parasitic elements of various types are placed between antenna elements, which can efficiently reduce mutual interference. Metamaterials have strong potential to alter surface waves [4] or change transmission modes [11]. In doing so, isolation is enhanced between ports/elements. Stacking a certain superstrate material over the array substantially reduces mutual coupling between the individual elements [12]. In [13] a Partial Reflecting Surface (PRS) is reported for mutual coupling reduction. Authors in [14] report a suspended metasurface constructed of repetitive square split ring resonators (SRRs) to accomplish decoupling for the two patch antennas.

Single layer design has been used to fabricate MIMO antennas, and these patch antennas have intrinsic limitations such as poor gain and restricted bandwidth [15]. A multi-layered structure is a regularly used strategy for overcoming these restrictions. The authors of [16] presented a dual-plane antenna array design for a multiband connection environment. However, the proposed design can achieve a 2 dB antenna gain.

WB or UWB antennas that use the defective ground approach have high radiation loss due to backward radiation. Novel designed meta-surfaces called Partial Reflecting Surfaces (PRS) have been widely documented to improve antenna gain [17]. A PRS is typically situated $\lambda/2$ away from the radiating layer. The described antenna in [17] tries to build a Fabry-Perot cavity with a parallel-plating arrangement. By substituting ground planes with Artificial Magnetic Conductors in [18], the distance between ground plane and PRS is lowered to $\lambda/4$. (AMCs). However, AMCs do not contribute considerably to producing a small design. In [19], PRS is positioned underneath the antenna, but only a 3 dB gain increase is reached. The design described in [20] only operate on a single frequency band. Overall, achieving increased electrical gain, reduced physical size, and multiband capability in multilayered systems is not easy. This article discusses an antenna design for M2M/ IoT applications requiring increased gain and multiband capabilities. A defective structure in the proposed design helps to achieve more than 15 dB isolation (S12/S21) among radiating devices over the whole ultra-wideband. To provide the second necessary functionality, the planned design also employs a PRS superstrate above the radiating elements. On whole ultra-wide band, the results show enhanced impedance match and increased gain.

The remainder of this paper is distributed in following sections: Section II presents model schematics, while Section III presents simulated outcomes. Section IV provides an analysis of PRS. Ultimately, Section V brings the paper to a close.

II. Symmetrical Design Of Proposed Array

The proposed 3-dimensional array is based on two layers. The antenna array is etched on the front and a ground plane is etched on the far side of the first layer. This layer is built on a 1.6 mm thick epoxy laminate FR-4 substrate. The second layer is made up of PRS. This layer is also made on a FR-4. The height of superstrate has been kept at $\lambda/4$. Schematics of prototype antenna are shown in fig.1.

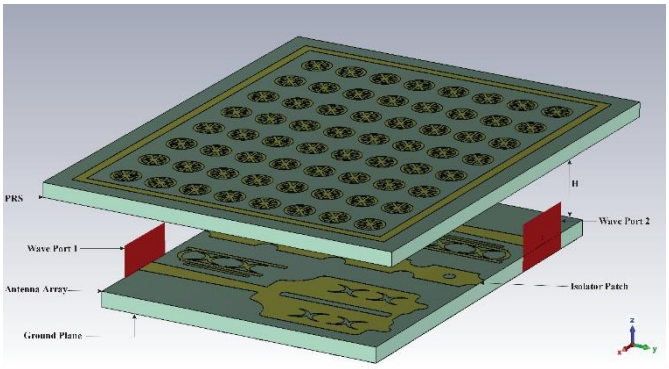

Fig. 1 3D layout of Proposed Structure

Antenna is excited by use of a 50-Ω microstrip feed line. The radiating element dimensions are $P_L \times D_3$. A capacitive parasitic strip containing cross hatch pattern inclusion is placed next to feedline, to achieve the overall impedance match as well as reduce mutual coupling between radiating elements. As this patch antenna is resonant at ultra-wide band (3.2-10.5GHz) therefore five defect slots are employed in each of main radiating element fig.2.

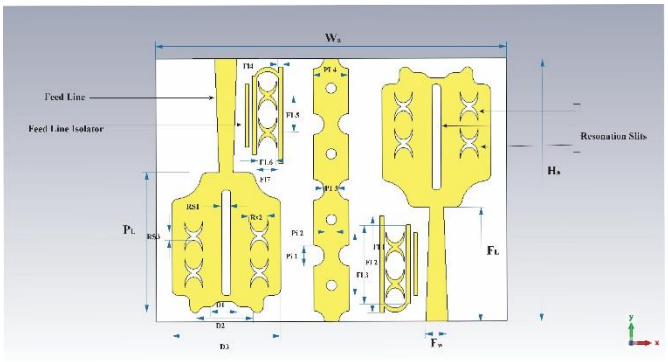

Fig. 2 Computer Aided Design of Layer 1 (Front View)

The Defective ground structure has been employed in combination with resonation slits to improve reflection coefficient and lower operational band fig.3.

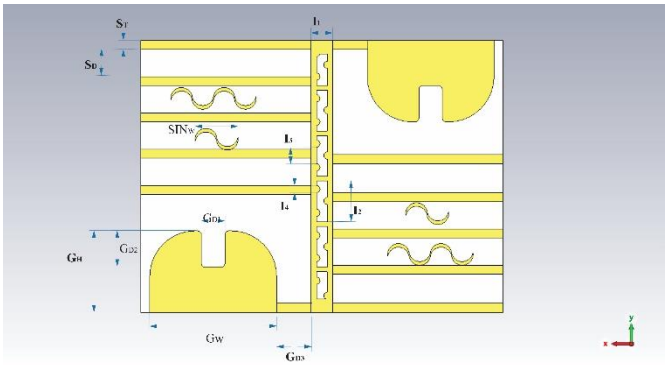

Fig. 3 Computer Aided Design of layer 1 (Back View)

III. Design And Simulated Computation

Superstrate comprises of PRS in the proposed array to achieve metasurface properties. These computationally expensive structures are analysed and optimized using CST MICROWAVE STUDIO® (CST MWS). The entire construction is contained in an open-air background, and the patch is powered by a wave port. To obtain credible simulation results, the entire structure is modelled in single computation, and no parallel boundary has been used for PRS. This section describes the architecture as well as the simulation findings.

A. *Proposed Radiating Element*

The slits etched in the patch are used to reduce size and achieve multi-resonant capability in the radiating structure [21]. This necessitates careful consideration of slit location and dimension. Current flow is reversed around the sides of horizontal slots. It produces the desired resonances. Impacts of etched slots on radiation coefficients of radiating elements can be seen on fig.4.
Resonance is mainly generated by vertical slit with a length of 12mm, while the succeeding cross hatch slots amplify its effect. The placement of all four cross hatch slots influences the position of resonance in the UWB band. To add the desired frequency range, the effective length of the slit is necessary. Equations (1) and (2) can be used to obtain dipping at appropriate frequency bands:

$$f_r = \frac{c}{4l\sqrt{\varepsilon_{eff}}} \quad (1)$$

$$\varepsilon_{eff} = \frac{\varepsilon_r + 1}{c} \quad (2)$$

where c is the speed of light, $\boldsymbol{f_r}$ is the desired spectrum's core frequency, and $\boldsymbol{\varepsilon_{eff}}$ is the dielectric substrate's permittivity, which is based on the dielectric contact $\boldsymbol{\varepsilon_r}$ of the substrate. The computed lengths of etched defects, as well as their relative position to feedline, define the range of frequencies to be added to the band of resonance.

Table 1. Geometric Measurements of Proposed Array

Parameters	mm	Parameters	mm
W	40	G_W	14
L	30	G_H	10
H	11	G_{D1}	3.6
P_L	12.4	G_{D2}	3.4
F_L	13	G_{D3}	3.8
F_W	2.5	I_1	2.4
F_{I1}	11	I_2	4.5
F_{I2}	8.83	I_3	1.8
F_{I3}	7.2	I_4	0.8
F_{I4}	0.5	S_T	1
F_{I5}	4.2	S_D	3
F_{I6}	2.07	SIN_W	4.7
F_{I7}	2.25	W_{PRS}	48
P_{I1}	2.4	L_{PRS}	38
P_{I2}	1.2	T	32
P_{I3}	1.5	U	42
P_{I4}	4	W_R	3
R_{S1}	1	X	0.3
R_{S2}	2.07	Y	0.83
R_{S3}	1.5	M_T	0.02
D_1	3.5	D_3	12.4
D_2	7	r(FR-4)	4.3
t(FR-4)	0.025	--	--

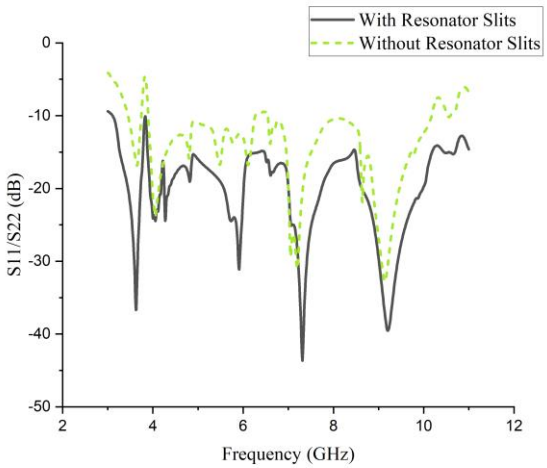

Fig. 4 Computed S-Parameters of array, with and without Slits

B. *Defected Ground Plane*

The dimensions and design of the defected ground plane influence the antenna's mode of excitation and resonance. The suggested array employs a defected ground plane, which aids in increasing the bandwidth of a patch antenna. It can be seen that the resonance weakens as the conventional ground plane is introduced. The trade off with partial ground is that some of energy is radiated back. Proposed antenna array has optimized ground plane with regular defects ensuring resonation over entire UWB. Fig.5 depicts the effects of defection of ground plane on ultrawide band resonance.

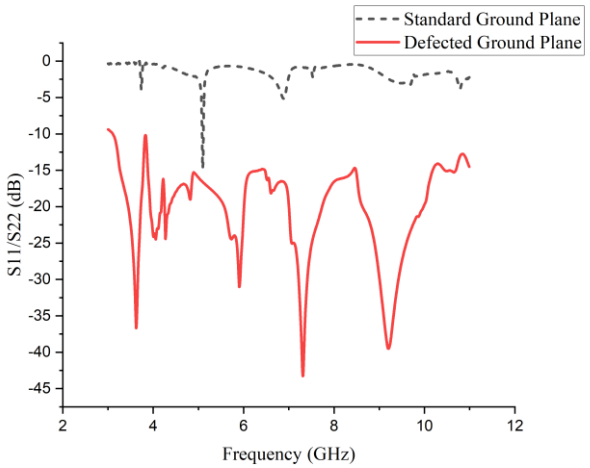

Fig. 5 Effects of ground plane defects on Return Loss

The horizontal slits placed just behind radiating structure act as reflectors for frequencies above 5GHz and sinosidal structures placed between slits are placed for resonace at 8GHz.

C. *Isolator Slits*

A cross hatch parasitic patch has been placed near feed lines of antennas as impedance match enhancer to mitigate the effects of defected ground. This structure along with center isolator is used to enhance the overall return loss. Center Isolator is placed between both radiating structures to reduce mutual coupling as well as maitain a positive return loss.

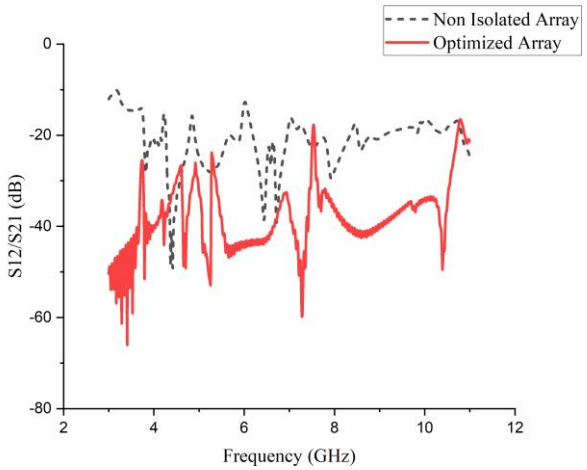

Fig. 6 Mutual Coupling of Array(with/without Isolator patch)

IV. PRS(PARTIAL REFLECTIVE SURFACE)

As illustrated in Fig. 6, the proposed PRS comprises direct etched eight-Pie cut circle patches organized in a square grid. T×U is the dimension of the square grid.

The PRS has an overall array size of 8×8 cells. W_{PRS}×L_{PRS} are the overall dimensions of PRS. Fig. 6 depicts the intended PRS dimensions. The size of these patches should be minimal to improve gain at higher frequencies. Conversely, to attain peak gain at low frequency, these patches need be kept larger in size. As a result, the unit-cell dimension is tuned to yield high gain on entire UWB. Table 1 exhibits the adjusted dimensions of the PRS unit cell.

The resonance requirement listed below must be met in order to compute the cavity height of the proposed PRS antenna.

$$H_r = \left(\frac{\lambda}{\pi} - 1\right)\frac{\lambda}{4} + N\frac{\lambda}{2}, \quad N = 0,1,2,\ldots.. \quad (3)$$

Optimal size of unit cell is also a necessary function of directivity $\boldsymbol{D}$ which can be written as function of reflection coefficient $\boldsymbol{\Gamma}$ of underlaying antenna.

$$D = 10.\log\left(\frac{1+|\Gamma|}{1-|\Gamma|}\right) \quad (4)$$

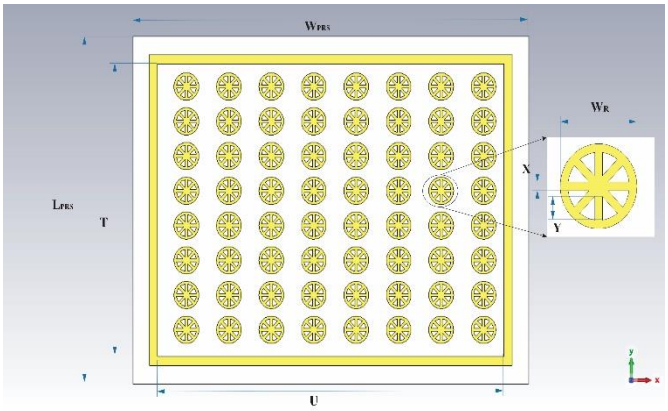

Fig. 6 Configration of PRS-Superstrate and Unit Cell

A. PRS Effects on Gain

The electromagnetic coupling or cavity effect generated between the PRS structure and the radiating patch results in gain amplification. Because of the Fabry-Perot effect, the PRS considerably increases the gain at both desired bands, as illustrated in Fig. 7. The average gain increment over entire band is around 3dB with peak gain at approximate 6.5 dB around 6GHz and 10GHz.

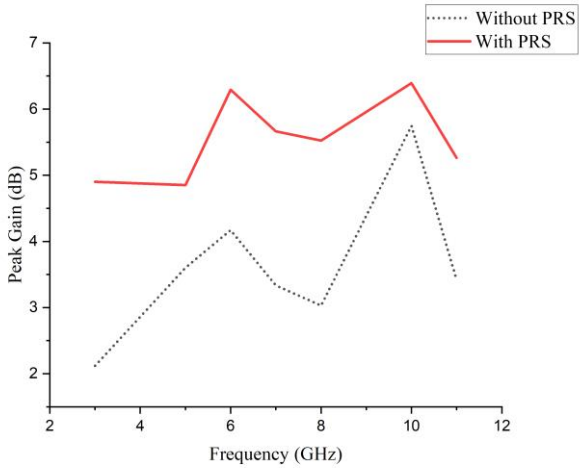

Fig. 7 Simulated Gain results with and without PRS

V. MEASURED RESULTS

This section analyses the measured outcomes of the built array. As illustrated in Fig. 9, a prototype with enhanced dimensions as listed in Tab.1 is produced and tested on a FR-4 Laminate substrate. The measurements were carried out on an Agilent PNA-X(N5242A), and the radiation patterns were measured with a DEPM equipment in an anerobic chamber.

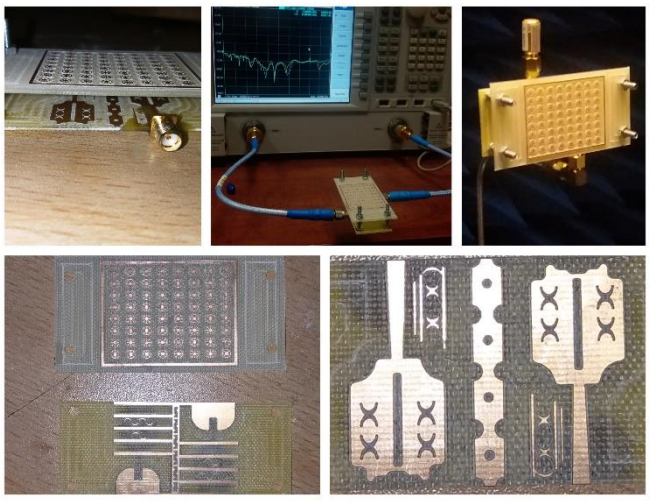

Fig. 8 Fabricated Prototype on Anerobic Test Stand

A. S-Parameter

Fig. 9 depicts the measured and modelled return loss of the array system. It may be established that the array is matched across Ultra-Wide band 3.5GHz-10.5GHz. The measured and simulated findings correlate with one another.

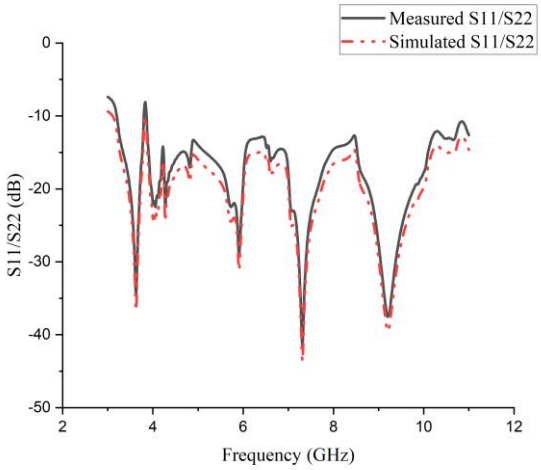

Fig. 9 Measured and Simulated Return Loss

B. Gain

Fig. 10 exhibits the measured and simulated gains of the proposed architecture. It is possible to see that the gains at 7-10GHz is 5dB. The 2-dB disparity between the measured and simulated findings is attributable to fabrication imperfections.

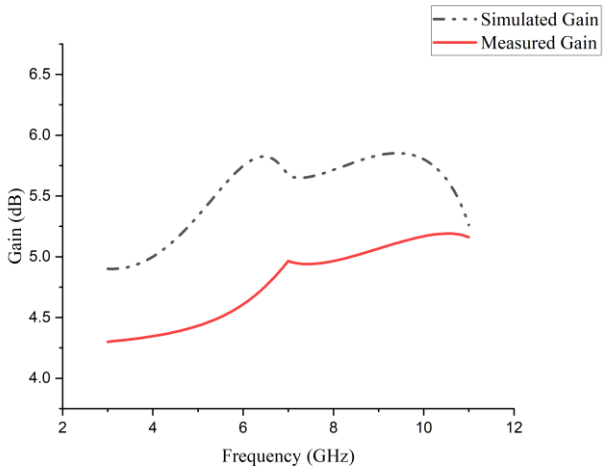

Fig. 10 Simulated and Measured Gain

C. Radiation Pattern

Fig. 11 illustrates the radiation patterns of the proposed architecture at UWB(3.5-10.5GHz). Sample measurment for E,H-plane has been shown in figure at frequencies for 3 GHz.5 GHz,7 GHz and 10GHz from top to bottom respectively. As a conventional strategy for achieving ultra wideband response, the antenna has a partial ground plane, and the radiation pattern has lobes in both the upper and lower directions. As the PRS is not supported by a solid ground plane, it exhibits the effects of beam steerability when traversing across the resonant band. The graph indicates clearly that the proposed PRS array exhibits good main lobe radiation and a significant gain.

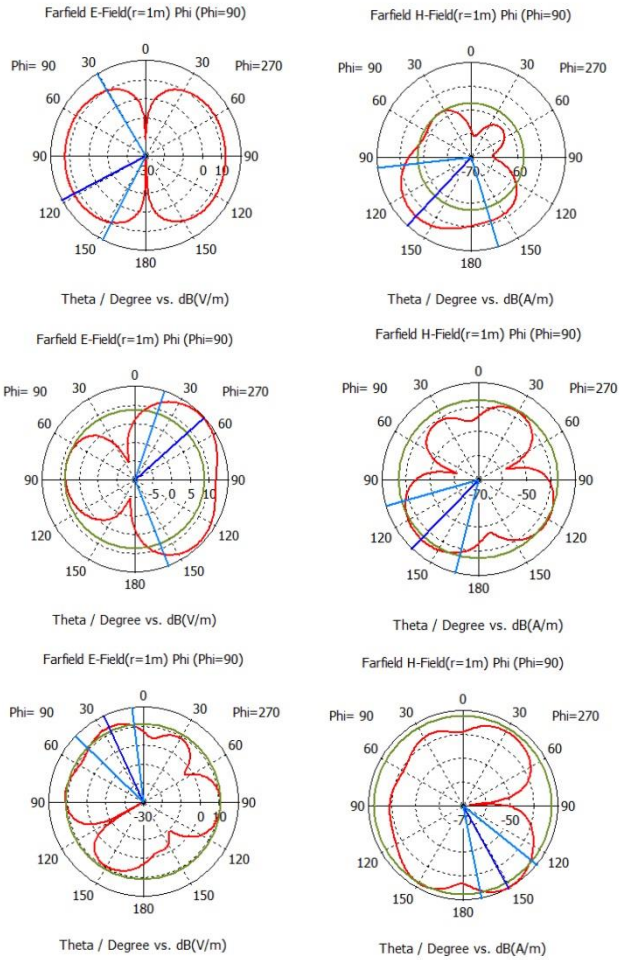

Fig. 11 Measured E-plane(Left) and H-plane(right)

VI. DISCUSSION

This section ilustrates the comparison of proposed prototype with reported techniques in exising literature. As Table data shows the proposed design has better frequency range than existing designs. Isolation between radiating elements is good as compared to other techniques allready implemented. Although there is a tradeoff in size of array antenna. The proposed design is a 3 dimensional array as it comprises of multiple

layers, so it is comparably bigger than techniques allready employed in 2D designs. In Comparison to existing 3D arrays proposed design is smaller.

Table 2. Comparison with Existing Literature

Ref no	F(GHz)	Isolation (dB)	Antenna Dimensions
[4]	3.5	>26.9	65×50 mm^2
[5]	2.3	>30	N/A
[6]	1.65	>40	98×65 mm^2
[13]	3.7-4.1	>30	48.5×60.6×18 mm^3
[14]	5.4-5.8	>15	40×26×9.3mm^3
Proposed Array	3.5-10.5	>50	38×48×11mm^3

VII. CONCLUSION

This work presents a compact PRS-based 2-layered, UltraWide-band array antenna with good gain in entire band 3.5GHz-10.5GHz. To achieve UWB operation, slots are added to the patch. To improve gain, the PRS layer is positioned above the antenna layer. The antenna has average band gain of 6dB. The measured and simulated findings are in good agreement, indicating that the array of antennas is suited for M2M communication, UWB high gain applications, and a wide services in electronic healthcare, and automated transportation.

REFERENCES

[1] L. D. Xu, W. He and S. Li, "Internet of things in Industries: A Survey," *IEEE Transactions on Indust-rial Informatics*, vol. 10, no. 4, pp. 2233-2243, 2014.

[2] K. Y.Yazdandoost and R. Miura, "Compact printed Multiband antenna for M2M applications," in *8th European Conference on Antennas and Propag-ation(EuCAP)*, 2014.

[3] M. Moosazadeh and S. Kharkovsky, "Compact and small planar monopole antenna with symmetrical L- and U-shaped slots for WLAN/WiMAX applica-tions," *IEEE Antennas and Wireless Propagation Letters*, vol. 13, pp. 388-391, 2014.

[4] J. Ghosh, D. Mitra and S. Das, "Mutual Coupling Reduction of Slot Antenna Array by Controlling Surface Wave Propagation," *IEEE Trans. Antennas Propag.*, vol. 67, no. 2, 2019.

[5] Y. L. a. S. G. H. Huang, "Uniplanar differentially driven UWB polarisation diversity antenna with band-notched characteristics," *Electronic Letters*, vol. 51, pp. 206-207, 2015.

[6] S. I. Jafri, R. Saleem, M. F. Shafique and a. A. K.Brown, "Compact reconfigurable multiple-inputmultiple-output antenna for ultra-wideband Applications," *IET Microwaves, Antennas & Prop.*, vol. 10, pp. 413-419, 2016.

[7] K. M. R. K. a. K. S. R. K. S. Vishvaksenan, "Mutual Coupling Reduction in Microstrip Patch Antenna Arrays Using Parallel Coupled-Line Resonators," *IEEE Antennas Wirel. Propag. Lett.*, vol. 16, 2017.

[8] L. Zhao and K.-L. Wu, "A Dual-Band Coupled Resonator Decoupling Network for two coupled antennas," *IEEE Trans. Antennas Propag.*, vol. 63, no. 7, 2015.

[9] K. Wei, J.-Y. Li, L. Wang, Z.-J. Xing and R. Xu, "Mutual Coupling Reduction by Novel Fractal Defected Ground Structure Bandgap Filter," *IEEE Trans. Antennas Propag.*, vol. 64, no. 10, 2016.

[10] K. Wei and B.-C. Zhu, "The Novel W Parasitic Strip for the Circularly Polarized Microstrip Antennas Design and the Mutual Coupling Reduction Between them," *IEEE Trans. Antennas Propag.*, vol. 27, no. 2, 2019.

[11] J. Guo, F. Liu, L. Zhao, Y. Yin, G.-L. Huang and Y.Li, "Meta-Surface Antenna Array Decoupling Designs for Two Linear Polarized Antennas Coupled in H-Plane and E-Plane," *IEEE Access*, vol. 7, 2019.

[12] M. Akbari, M. M. Ali, M. Farahani, A. R. Sebak and T. Denidni, "Spatially Mutual coupling reduction between CP-MIMO antennas using FSS superstrate," *Electronic Letters*, vol. 53, no. 08, 2017.

[13] S. Bibi, R. Saleem, A. Q. 2, S. u. Rehman and M. F. Shafique, "Dual-Band Antenna for High Gain M2M Communication Using PRS," *ACES* , vol. 32, no. 11, 2017.

[14] Z. H. Jiang, P. E. Sieber, L. Kang and D. H. Werner, "Restoring Intrinsic Properties of Electromagnetic Radiators Using Ultralightweight Integrated Metasurface cloaks," *Adv. Funct. Mater*, vol. 25, no. 29, 2015.

[15] Z. Liu, J.Wang, S.Qu, J.Zhang, H.Ma, Z.Xu and A.Zhang., "Enhancing isolation of antenna arrays by

simultaneously blocking and guiding magnetic field lines using megnatic metamaterials," *Appl. Phys. Lett.*, vol. 109, no. 15, 2016.

[16] X. Tan, W. Wang, Y. Wu, Y. Liu and A. A. Kishk, "Enhancing Isolation in DualBand Meander-Line Multiple Antenna by Employing Split EBG Structure," *IEEE Trans. Antennas Propag.*, vol. 67, no. 4, 2019.

[17] D. S. S. N. B. a. A. d. L. D. Germain, "Phase-compensated metasurface for a conformal microwave antenna," *Applied Physics Letters*, vol. 102, no. 12, 2013.

[18] F. C. a. F. D. F. A. Hosseini, "Gain enhancement of a V-band antenna using a Fabry-Pérot cavity with a self-sustained all-metal cap with FSS," *IEEE Transactions on Antennas and Propagation*, vol. 63, no. 3, pp. 909-921, 2015.

[19] M.-C. Tang, Z.Chen, H.Wang, B. M.Li, J.Wang, Z.Shi and R. Ziolkowski, "Mutual Coupling Reduction Using Meta-Structures for Wideband, DualPolarized, and High-Density Patch Arrays," *IEEE Trans. Antennas Propag.*, vol. 65, no. 08, 2017.

[20] K.-L. Wu, C. Wei, X. Mei and Z.-Y. Zhang, "Array-Antenna Decoupling Surface," *IEEE Trans. Antennas Propag.*, vol. 65, no. 12, 2017.

[21] A. A. e. al., "Isolation improvement in UWB-MIMO antenna system using slotted stub," *Electronics*, p. 1582, 2020.

[22] S. M. R. Islam, D. Kwak, M. H. Kabir and M. Hossain, "The Internet of things for Healthcare: A comprehensive Survey," *IEEE Access*, vol. 3, pp. 678-708, 2015.

[23] M. Farahani, J. Pourahmadazar, M. Akbari, M. Nedil, A. R. Sebak and T. A.Denidini, "Mutual Coupling Reduction in Millimeter-Wave MIMO Antenna Array Using a Metamaterial Polarization-Rotator Wall," *IEEE Antennas Wirel. Propag. Lett.*, vol. 16, 2017.